Current affiliation: University of Leeds, Leeds, UK.

Constrained $1\frac{1}{2}$-Layer Hamiltonian Toy Models for Stratospheric Dynamics*

By Onno Bokhove†

Department of Applied Mathematics, University of Twente, The Netherlands
Institute of Mechanics, Processes and Control—Twente

Summary

A two-layer Hamiltonian toy model consisting of two isentropic stratospheric layers is simplified using perturbation analysis while preserving the Hamiltonian structure. These two layers are neutrally and stably stratified. The first approximation applies when the Froude number of the upper isentropic layer is small, such that the upper surface is approximately rigid, and this upper layer is much thicker than the lower layer. A conservative $1\frac{1}{2}$-layer isentropic model emerges when leading-order perturbation theory is used in the Hamiltonian formulation of the isentropic two-layer model. Furthermore, Hamiltonian theory directly leads to (Salmon's) L1-dynamics for the novel $1\frac{1}{2}$-layer model, following a more concise derivation than shown before, when the Rossby number in the upper stratospheric layer is small and leads to a geostrophic constraint.

Keywords: $1\frac{1}{2}$-layer toy model isentropic layers Hamiltonian formulation perturbation theory rigid-lid constraint nearly geostrophic constraints

1. Introduction

Numerical weather prediction (NWP) is based on a space and time discretization of a dynamical system of partial differential equations for the dynamics of the atmosphere in combination with a data analysis of atmospheric observations. These observations are distributed in space and time. The elaborate step involving the data analysis is required to provide an initial condition for the dynamical system such that stable and realistic solutions result thereafter. Without a reasonably proper analysis and initialization, the resulting numerical integration exhibits unrealistic gravity-wave oscillations (*e.g.*, Daley, 1991).

To understand why these unwanted unrealistic oscillations arise (and for many more other reasons), meteorologists have explored simplified dynamical systems of the atmosphere, ranging from finite-dimensional to infinite-dimensional systems, rather than the "primitive" three-dimensional rotating compressible Navier-Stokes equations (e.g. Bokhove, 2002b; Vanneste, 2004; Vanneste and Yavneh, 2004; and references therein). The latter equations are commonly accepted as a valid starting point even though multiphase aspects of the atmosphere due to the presence of water in its various phases, chemicals and aerosols may require more complicated modeling. This tendency to study simplified or balanced models of the atmosphere to gain (theoretical) insights runs in parallel with the history of NWP. The first computerized NWP by Charney et al. (1950) used the equivalent barotropic vorticity equation, which is a severe simplification of the above-mentioned primitive equations. It does, however, capture leading-order aspects of the large scale dynamics, such as the basic evolution of barotropic high and low pressure systems, because the large-scale dynamics is in approximate hydrostatic and geostrophic balance. Hydrostatic balance is often a valid approximation on larger scales because the atmosphere is thin with a small aspect ratio between vertical spatial and velocity scales, and the horizontal ones. In turn, geostrophic balance is approximately valid as the large scale wind in the

* with an Appendix "Slaved Hamiltonian Dynamics" by O. Bokhove and T.G. Shepherd.

† Department of Applied Mathematics, University of Twente, P.O. Box 217, 7500 AE Enschede,The Netherlands; o.bokhove@math.utwente.nl

extratropics is often aligned roughly parallel to pressure contours at a certain height.

In these studies of simplified models and in their construction much emphasis has been placed on the preservation of conservation laws present in the inviscid system (Lorenz, 1960). Their preservation often does stabilize and constrain solutions in (discretized) phase space. The barotropic vorticity equation used by Charney et al. (1950) is an example of a conservative, Hamiltonian balanced model (Shepherd, 1990) in which the potential vorticity is materially advected while the winds follow from the potential vorticity via an inversion of an elliptic equation. The presence of these integral or flux conservation laws, then, is intimately related to the existence of a Hamiltonian structure of many dynamical fluid systems (see the review by Shepherd, 1990; and the book by Salmon, 1998).

Layer models of the atmosphere and oceans are common simplifications of the Navier-Stokes or Euler equations in which the assumptions of hydrostatic balance and the discretization of the stratification (in the vertical) into intervals with piecewise constant values of the density or entropy have been explored (*e.g.*, Ripa, 1993; Salmon, 1998; and, Bokhove, 2002a). Layers with actual piecewise constant entropy are at best neutrally stable provided that the entropy increases upward from layer to layer. In contrast, the troposphere and especially the stratosphere generally have significant stable stratification. This makes isentropic layer models a poor representation of the atmosphere, and these models can only be used as toy models at best, on the one hand. We will use (two-layer) isentropic toy models solely as a means for the presentation of a leading-order Hamiltonian perturbation theory, and *not* as realistic prediction models. On the other hand, we may also view isentropic layer models simply as a crude, leading order finite volume discretization of the entropy in the vertical. The piecewise constant values of the entropy can simply be seen as mean values, resulting from projections onto locally constant test functions, of monotonically increasing entropy profiles in the respective layers. The implicit understanding is then that each isentropic layer approximates a stably stratified atmosphere with increasing entropy values in the vertical.

In models with $n+1$ isentropic layers, the vertical position of the top surface of the last layer is time dependent, while in the corresponding $(n+\frac{1}{2})$-layer model this surface is held rigid. In contrast to classic isopycnic models, isentropic models do not require the additional constraint of incompressibility, which may be more appropriate since the troposphere coupled to a deep stratosphere is compressible. Pressure coordinates are often used in the vertical but these introduce an effective incompressibility constraint that is (slightly) less ideal in a Hamiltonian formulation. The present goal, then, is to derive a consistent Hamiltonian formulation of a $1\frac{1}{2}$-layer isentropic toy model as a simple conceptual atmospheric model with an active thin lower stratospheric layer and a driven, thick upper stratospheric layer as well as gravity-wave motion.

The atmosphere at mid-latitudes can roughly be divided into a troposphere with a layer thickness of about 11 km from the Earth's surface to the tropopause, and a stratospheric layer reaching from 11 km to about 50 km. In a simplified view of atmospheric dynamics, the dynamics (below 50 km) can be presented into three isentropic layers with different but constant mean values of the entropy. The tropospheric layer ranges from 0 to about 10.6km, the first stratospheric layer from about 10.6 to 16.6km, and the second stratospheric layer from circa 16.6 to 34.6km. For algebraic simplicity, the tropospheric layer and the tropopause

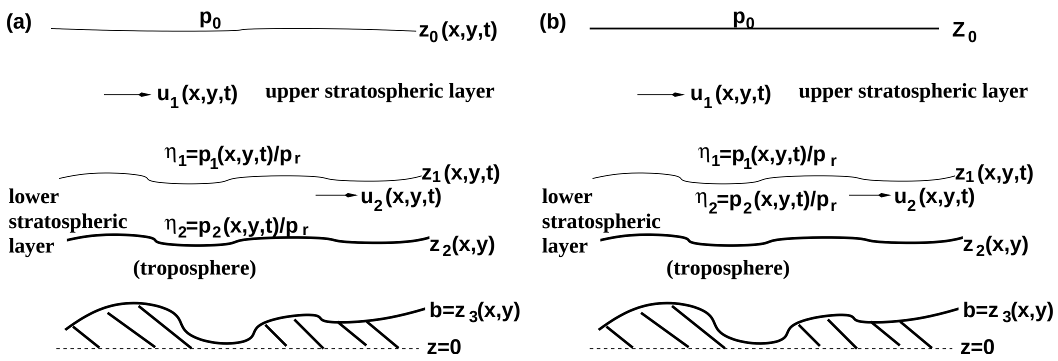

Figure 1. Sketch of part of the atmosphere with isentropic stratospheric upper and lower layers and the associated variables. The tropospheric layer is ignored here for simplicity. (a) In the two-layer model, the interface at $z = z_1(x, y, t) \approx 18$km between the upper and lower layers and the top surface of the upper stratospheric layer at $z = z_0(x, y, t) \approx 36$km are time dependent. (b) In the $1\frac{1}{2}$-layer model, this top surface at $z_0 = Z_0$ is held rigid and we assume further that the upper layer is much thicker than the lower stratospheric layer. An aim of this paper is to derive a consistent, Hamiltonian $1\frac{1}{2}$-layer model from a stratospheric two-layer model.

are held fixed to focus entirely on the stratospheric dynamics (this condition is easily lifted without harming the arguments presented in this paper). To ensure static stability, the entropy value of the upper stratospheric layer, θ_1, must be larger than the value in the lower stratospheric layer, θ_2. Again, we could assume implicitly that the layers are stably stratified such that the entropy is increasing upward. The values θ_1 and θ_2 are then to be interpreted as the mean projections of the increasing entropy in the lower and upper stratospheric layer. Using hydrostatic balance and considering a horizontal velocity field that is vertically uniform in each layer, the dynamics remains horizontal in each layer with a (weak) coupling between the layers (*e.g.*, Salmon, 1998; and Bokhove, 2002a). Such simplified, toy models can be analyzed in much more detail than the primitive three-dimensional equations of motion, and play and have played a major role in gaining understanding of the atmosphere's dynamics (*e.g.*, Starr, 1945; Verkley, 2001; and Trieling and Verkley, 2003; concerning isentropic models).

(*a*) *Equations of motion*

Using z as the vertical coordinate, the second, lower stratospheric layer reaches from the tropopause here simplified to be static at $z = z_2(x, y) \approx 10.63$km with pressure $p_2(x, y, t)$ to the first stratospheric dynamic interface at $z = z_1(x, y, t) \approx 16.63$km with pressure $p_1(x, y, t)$. Here x and y are horizontal coordinates and t is time. The first, upper layer reaches from the interface at $z = z_1$ to the top, dynamic interface at $z = z_0(x, y, t) \approx 34.63$km where the pressure p_0 is constant, see also the defining sketch in Fig. 1(a). In the two-layer model, the top of the first layer is a time dependent surface. In contrast, for the $1\frac{1}{2}$-layer model to be derived the top surface is constrained to be constant, that is, $z_0 = Z_0$ with Z_0 the appropriate constant, see Fig. 1(b). The upper layer is subsequently counted as a half layer.

A derivation of a three-layer model is given in a companion paper by Bokhove and Oliver (2007). The two-layer model considered here arises as a simplification thereof by ignoring the dynamics in the third, tropospheric layer, as sketched in

Fig. 1. The momentum equations of the model result by using hydrostatic balance and the constancy of entropy in the respective layers. The continuity equations emerge by using the pseudo-density $\sigma_\alpha(x, y, t)$ in each layer α. This pseudo-density arises when we use hydrostatic balance $\mathrm{d}p = -\rho\, g\, \mathrm{d}z$ to integrate an element of mass $\mathrm{d}m = \rho\, \mathrm{d}x\, \mathrm{d}y\, \mathrm{d}z = -\mathrm{d}x\, \mathrm{d}y\, \mathrm{d}p/g$ across each layer with density ρ, pressure p, and the gravitational acceleration g. Ripa (1993) and Bokhove (2002a) derive the variational and Hamiltonian formulation of (isentropic) layer equations directly (by simplifying the Eulerian variational principle of the compressible Euler equations). The resulting isentropic two-layer equations (Bokhove and Oliver, 2007) are

$$\begin{aligned}\frac{\partial \sigma_\alpha}{\partial t} + \boldsymbol{\nabla}\boldsymbol{\cdot}(\sigma_\alpha\, \mathbf{v}_\alpha) = 0\\ \frac{\partial \mathbf{v}_\alpha}{\partial t} + (\mathbf{v}_\alpha \boldsymbol{\cdot} \boldsymbol{\nabla})\mathbf{v}_\alpha + \mathsf{f}\, \mathbf{v}_\alpha^\perp = -\boldsymbol{\nabla} M_\alpha\end{aligned} \tag{1}$$

with $\alpha = 1$ in the upper and $\alpha = 2$ in the lower layer, horizontal gradient $\boldsymbol{\nabla}$, the pseudo-densities $\sigma_1 = p_r\,(\eta_1 - \eta_0)/g$ and $\sigma_2 = p_r\,(\eta_2 - \eta_1)/g$ in the upper and lower layer defined as the dimensionless pressure difference over the layer divided by g, the horizontal velocity $\mathbf{v}_\alpha = \mathbf{v}_\alpha(x, y, t) = (u_\alpha, v_\alpha)^T$ in layer α, $\mathbf{v}^\perp = (-v, u)^T$, a constant Coriolis parameter f, and the Montgomery potential M_α. Here we used the dimensionless pressure $\eta = p/p_r$ with reference pressure p_r. In the (stratospheric) lower layer with thickness $h_2 = z_1 - z_2$, the potential M_2 is related to p_2 and hence σ_1 and σ_2 as follows

$$M_2 = c_p\, \theta_2\, \eta_2^\kappa + g\, z_2 = g\, \big(h_2 + \frac{\theta_2}{\theta_1}\, h_1 + z_2\big) + c_p\, \theta_2\, \eta_0^\kappa, \tag{2}$$

where $\kappa = R/c_p$, the gas constant $R = c_p - c_v$, and c_p and c_v are the specific heats at constant pressure and volume, respectively; and, θ_2 is the constant potential temperature in the second layer. The equations of motion of an active, first layer with thickness $h_1 = z_0 - z_1$ are (1) for $\alpha = 1$, where the Montgomery potential

$$\begin{aligned}M_1 &= g\,(z_0 - Z_0) = g\,(h_1 + h_2 + z_2 - Z_0)\\ &= c_p\, \theta_2\, \eta_2^\kappa + c_p\,(\theta_1 - \theta_2)\, \eta_1^\kappa - c_p\, \theta_1\, \eta_0^\kappa + g\,(z_2 - Z_0)\end{aligned} \tag{3}$$

with θ_1 the constant potential temperature in the upper layer. When the two-layer model covers a large part of the stratosphere it seems appropriate to take $\eta_0 = p_0/p_r \approx 0$. The top of the upper layer then has zero temperature which is unrealistic. We must therefore limit the vertical extent of our two-layer model to ensure that $\eta_0 > 0$. One may show that in the $1\frac{1}{2}$-layer model the stratospheric momentum equations reduce to $M_1 = g\,(z_0 - Z_0) = 0$. Hence, the top surface is fixed such that $z_0 = Z_0$. For the $1\frac{1}{2}$-layer model, the momentum equations in the lower stratospheric layer remain (1) for $\alpha = 2$. The model is indeed closed, because $M_1 = 0$ defines p_1 in terms of p_2, which can then also be expressed in terms of σ_2 using $\sigma_2 = p_r\,(\eta_2 - \eta_1)/g$. We note that such a $1\frac{1}{2}$-layer model has the advantage over a one-layer model that the pressure p_1 is active and not constrained to be constant, as is p_0. Furthermore, the values of the surface pressure p_2 are more realistic.

The $1\frac{1}{2}$-layer model, however, seems inconsistent, since the constraint $M_1 = 0$ is not preserved in time by the original two continuity equations. Nevertheless, the closed $1\frac{1}{2}$-layer model (1) with $\alpha = 2$ and Montgomery potential M_2 results after taking $M_1 = 0$ and $\mathbf{v}_1 = 0$ in the momentum equation of the stratospheric layer.

(*b*) *Questions*

With (idealized) modeling using simplified or balanced models as further motivation, we arrive at the following key questions: (i) Can the inconsistency in the derivation of this $1\frac{1}{2}$-model be resolved? (ii) Can we construct a Hamiltonian formulation of the $1\frac{1}{2}$-layer model? (iii) Can we subsequently derive nearly geostrophic balanced models? Multilayer extensions of these (balanced) half-layer models with a passive upper layer can be readily derived, but the $1\frac{1}{2}$-layer model used here is arithmetically simpler, and suffices to explain a systematic, Hamiltonian approach.

Regarding the first question, (i), it can be answered adequately by applying asymptotic analysis to the above two-layer system and by extending a finite-dimensional slaved Hamiltonian approach, detailed in Appendix A, to an infinite-dimensional case. To answer the second question, (ii), we can use the Poisson bracket of the shallow water equations (e.g., Bokhove and Oliver, 2006), and search ad hoc for the potential energy that yields the desired Montgomery potential M_2. Perhaps not surprisingly, the original potential energy of the two-layer model subject to the constraint $M_1 = g\,(z_0 - Z_0) = 0$ does give the desired potential energy of the $1\frac{1}{2}$-layer model. The answer to the final question follows subsequently from the work of Vanneste and Bokhove (2002). Here we show that a slaved Hamiltonian approach provides a more concise derivation of balanced models, including Salmon's L1-dynamics, based on velocity constraints.

The use of two isothermal layers allows a stable representation within and between the layers. On the one hand, it could resolve the tenuous relevance of a two-layer isentropic atmosphere considered here. On the other hand, two isothermal layers can not be maintained without implicit forcing and dissipation even though the dynamics of a model with two isothermal layers itself is conservative and has a Hamiltonian formulation. Because the question on the maintenance of isothermal layers is presently unresolved, such a two-layer model is also questionable. The techniques presented in this paper can, however, be applied directly to such a two-layer isothermal model (for a three-layer model with isentropic (tropospheric) lowest layer and two (stratospheric) upper layers, see Bokhove and Oliver, 2007).

The paper outline is as follows. The Hamiltonian formulation of the $1\frac{1}{2}$-layer model is derived in a systematic manner in §2 by using a slaved Hamiltonian approach for continuous systems. Subsequently, in §3, we also construct the Hamiltonian formulation of balanced models for general velocity constraints (*cf.*, Vanneste and Bokhove, 2002) with a L1-balanced model (*cf.*, Salmon, 1985) as particularization for the $1\frac{1}{2}$-layer isentropic model. Although the latter derivations of nearly geostrophic balanced models are not novel, the presented derivation is Hamiltonian and more concise than the derivations in Salmon (1985, 1988), Allen and Holm (1996), Verkley (2001), McIntyre and Roulstone (2002), and Vanneste and Bokhove (2002). Consequently, the derivation of other Hamiltonian balanced models may be easier. Summary and discussion are found in §4.

2. $1\frac{1}{2}$-layer stratospheric isentropic model

(*a*) *On the two-layer equations*

The extra-tropical atmospheric model consists of a lower and an upper stratospheric layer, each with constant but different values of entropy. A derivation of the Hamiltonian three-layer model is given in Bokhove and Oliver (2007); the present two-layer model immediately follows as a simplification thereof.

For an ideal gas

$$p = \rho\, R\, T \tag{4}$$

with temperature T. In combination with a rewritten law of thermodynamics $T\, ds = c_p\, \mathrm{d}T - \mathrm{d}p/\rho$, we derive

$$T/\theta = \eta^{\kappa}, \tag{5}$$

where s is the entropy, $\theta = T_0\, e^{(s-s_0)/c_p}$ the potential temperature, $\eta = p/p_r$ with $p_r = 1000$mb, s_0 and T_0 reference pressure, entropy and temperature values.

Consider two isentropic stratospheric layers one ranging from $z_2(\boldsymbol{x}) \leqslant z < z_1(\boldsymbol{x}, t)$ and one from $z_1(\boldsymbol{x}) \leqslant z \leqslant z_0(\boldsymbol{x}, t)$. For any fluid parcel in an isentropic fluid column in each stratospheric layer, the pressure gradient plus gravitational term in the three-dimensional momentum equations become the following, after using (4) and (5),

$$\frac{1}{\rho}\, \boldsymbol{\nabla} p + \boldsymbol{\nabla}(g\, z) = \boldsymbol{\nabla}(\theta\, \Pi + g\, z) = \boldsymbol{\nabla} M, \tag{6}$$

since $\theta = \theta_2$ is constant and with Exner function $\Pi = c_p\, \eta^{\kappa}$. Hydrostatic balance is then $\partial M/\partial z = 0$ and integration of this relation from z_2 to $z < z_1$ expresses the Montgomery potential M in terms of the dimensionless pressure $\eta_2(x, y, t)$ at the (tropopause) height z_2 (fixed here for simplicity), to obtain

$$M = c_p\, \theta_2\, \eta^{\kappa} + g\, z = M_2 = c_p\, \theta_2\, \eta_2^{\kappa} + g\, z_2. \tag{7}$$

Likewise, for any fluid parcel in an isentropic fluid column in the upper stratospheric layer, the result is, using (4),

$$\frac{1}{\rho}\, \boldsymbol{\nabla} p + \boldsymbol{\nabla} g\, (z - Z_0) = \boldsymbol{\nabla}\big(\theta\, \Pi + g\, (z - Z_0)\big) = \boldsymbol{\nabla} M, \tag{8}$$

where we introduced an integration constant fixed to $-g\, Z_0$ for later convenience, and $\theta = \theta_1$ is constant. Integration of hydrostatic balance $\partial M/\partial z = 0$ from $z_1 < z$ to z_0 gives

$$M = c_p\, \theta_1\, \eta^{\kappa} + g\, (z - Z_0) = c_p\, \theta_1\, \eta_0^{\kappa} + g\, (z_0 - Z_0), \tag{9}$$

in which $\eta_0 = p_0/p_r > 0$ is passive and fixed but $z_0 = z_0(x, y, t)$ is variable. Evaluation of (9) at z_1 gives a relation

$$g\, z_0 = c_p\, \theta_1\, (\eta_1^{\kappa} - \eta_0^{\kappa}) + g\, z_1 \tag{10}$$

in terms of η_1 and $g\, z_1$. Evaluation of (7) at z_1 gives

$$g\, z_1 = c_p\, \theta_2\, (\eta_2^{\kappa} - \eta_1^{\kappa}) + g\, z_2 \tag{11}$$

in terms of η_1, η_2 and z_2. Hence, we find

$$g\, z_0 = c_p\, \theta_1\, (\eta_1^{\kappa} - \eta_0^{\kappa}) + c_p\, \theta_2\, (\eta_2^{\kappa} - \eta_1^{\kappa}) + g\, z_2$$

and from (9) the desired expression for the Montgomery function in the stratosphere, equaling M up to a constant,

$$M_1 = c_p\,\theta_1\,(\eta_1^\kappa - \eta_0^\kappa) + c_p\,\theta_2\,(\eta_2^\kappa - \eta_1^\kappa) + g\,(z_2 - Z_0) = g\,(z_0 - Z_0). \tag{12}$$

The thickness of each layer follows directly from (10) and (11) as

$$h_2 = z_1 - z_2 = \frac{c_p\,\theta_2}{g}\,(\eta_2^\kappa - \eta_1^\kappa) \quad \text{and} \quad h_1 = z_1 - z_0 = \frac{c_p\,\theta_1}{g}\,(\eta_1^\kappa - \eta_0^\kappa). \tag{13}$$

We next assume that the thickness of the lower layer is smaller than that of the upper layer, *e.g.*, $z_0 \approx Z_0 = 36$km, $z_1 \approx Z_1 = 18$km and $z_2 \approx Z_2 = 12$km. The asymptotic limit

$$\delta_a = (Z_1 - Z_2)/(Z_0 - Z_1) \equiv H_2/H_1 \ll 1 \tag{14}$$

then arises with $h_1 \approx H_1$ and $h_2 \approx H_2$. One finds from (13) and (14) approximately that $\theta_1\,(p_1^\kappa - p_0^\kappa) \gg \theta_2\,(p_2^\kappa - p_1^\kappa)$. Finally, the relation between layer pressure and pseudo-densities is

$$\eta_1 = g\,\sigma_1/p_r + \eta_0 \qquad \text{and} \qquad \eta_2 = g\,(\sigma_1 + \sigma_2)/p_r + \eta_0. \tag{15}$$

(*b*) *Scaling of the two-layer equations*

First, equations (1) are scaled as follows

$$\begin{aligned}
&(x, y) = L\,(x^*, y^*), \quad t = (L/U_2)\,t^*, \quad \mathbf{v}_\alpha = U_\alpha\,\mathbf{v}_\alpha^*, \quad M_\alpha = g\,H_\alpha\,M_\alpha^*,\\
&\quad \sigma_1 = (p_r/g)\,\sigma_1^* = (p_r/g)\,(\Sigma_1 + \varepsilon^2\,\sigma_1'), \quad \sigma_2 = \varepsilon^2\,(p_r/g)\,\sigma_2^*,\\
&\quad p_\alpha = p_r\,p_\alpha^*, \quad \theta_\alpha = (g\,H_1/c_p)\,\theta_\alpha^*, \quad h_\alpha = H_\alpha\,h_\alpha^*,\\
&\quad Z_0 = H_1\,Z_0^*, \quad \text{and} \quad z_2 = F_2^2\,H_2\,z_2^*
\end{aligned} \tag{16}$$

with horizontal length scale L; layer velocity and depth scales U_α and H_α; layer Froude numbers $F_\alpha^2 = U_\alpha^2/(g\,H_\alpha)$; $U_1/U_2 = \sqrt{F_1} = \varepsilon$; and, $\delta_a\,F_2^2 = \varepsilon^2$. The ratio δ_a of layer thicknesses and the ratio ε of layer velocities are assumed small. The Froude number in each layer is introduced because these numbers naturally appear in the scaling. After dropping the asterisks, the scaling (16) substituted in (13) yields

$$\begin{aligned}
h_1 =& \theta_1\,(\eta_1^\kappa - \eta_0^\kappa) = \theta_1\,(\sigma_1^\kappa - \eta_0^\kappa) \quad \text{and}\\
h_2 =& \frac{\theta_2}{\delta_a}\,(\eta_2^\kappa - \eta_1^\kappa) = \frac{\theta_2}{\delta_a}\,\big((\sigma_1 + \varepsilon^2\,\sigma_2)^\kappa - \sigma_1^\kappa\big),
\end{aligned} \tag{17}$$

in which we take $c_p\,\theta_1/(g\,H_1) = \mathcal{O}(1)$. Substituting (16) into (1), (2) and (3); using (17); dropping the asterisks on the scaled variables; and some reordering yields the following dimensionless and generic form of the equations of motion (cf. (A.16) in Appendix A)

$$\begin{aligned}
\frac{\partial \sigma_1'}{\partial t} + \varepsilon\,\boldsymbol{\nabla}\boldsymbol{\cdot}(\sigma_1'\,\mathbf{v}_1) + \frac{1}{\varepsilon}\,\boldsymbol{\nabla}\boldsymbol{\cdot}(\Sigma_1\,\mathbf{v}_1) &= 0\\
\frac{\partial \mathbf{v}_1}{\partial t} + \varepsilon\,\Big(\mathbf{v}_1\boldsymbol{\cdot}\boldsymbol{\nabla}\mathbf{v}_1 + \frac{1}{R_1}\,\mathbf{v}_1^\perp\Big) + \frac{1}{\varepsilon}\,\boldsymbol{\nabla} M_1' &= 0\\
\frac{\partial \sigma_2}{\partial t} + \boldsymbol{\nabla}\boldsymbol{\cdot}(\sigma_2\,\mathbf{v}_2) &= 0\\
\frac{\partial \mathbf{v}_2}{\partial t} + \mathbf{v}_2\boldsymbol{\cdot}\boldsymbol{\nabla}\mathbf{v}_2 + \frac{1}{R_2}\,\mathbf{v}_2^\perp + \boldsymbol{\nabla} M_2' &= 0
\end{aligned} \tag{18}$$

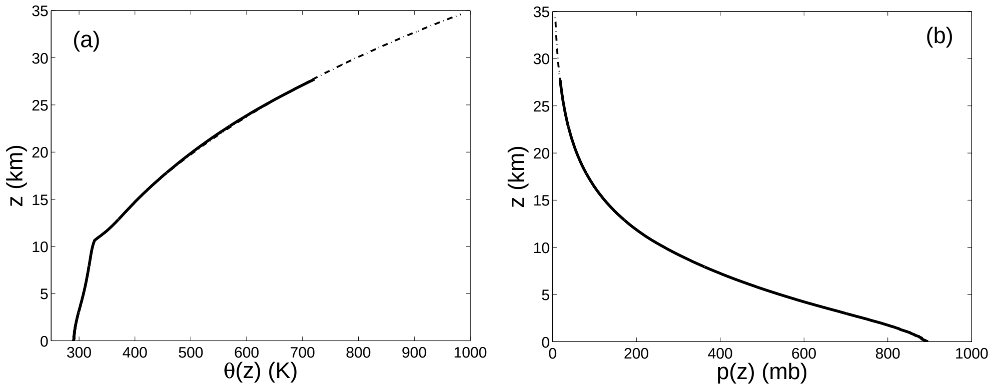

Figure 2. Profiles, zonally averaged, (solid lines) of observed potential temperature $\theta(z)$ and pressure $p(z)$ versus height z at circa 57.25°N, and extrapolated profiles (dash-dotted lines) from $Z_1 = 16.63$km to $Z_0 = 34.63$km based on the approximately constant scale heights of the observed θ and p, respectively, in the stratosphere. The tropopause lies at approximately $Z_2 = 10.63$km. Figure courtesy of Dr. Thomas Birner, University of Toronto (cf. Birner, 2006).

with potentials

$$\begin{aligned} M_1' &= \left(M_1 - \theta_1\,(\Sigma_1)^\kappa + Z_0 + \theta_1\,\eta_0^\kappa\right)/\varepsilon^2 = \theta_1\,\left((\Sigma_1 + \varepsilon^2\,\sigma_1')^\kappa - (\Sigma_1)^\kappa\right)/\varepsilon^2 \\ &\qquad + \theta_2\,\left((\Sigma_1 + \varepsilon^2\,\sigma_1' + \varepsilon^2\,\sigma_2)^\kappa - (\Sigma_1 + \varepsilon^2\,\sigma_1')^\kappa\right)/\varepsilon^2 + z_2, \\ M_2' &= M_2/F_2^2 - \theta_2\,\Sigma_1^\kappa/\varepsilon^2 \\ &= \theta_2\,\left((\Sigma_1 + \varepsilon^2\,\sigma_1' + \varepsilon^2\,\sigma_2)^\kappa - (\Sigma_1)^\kappa\right)/\varepsilon^2 + z_2, \end{aligned} \tag{19}$$

Rossby numbers $R_\alpha = U_\alpha/(\mathsf{f}\,L)$, and $\delta_a = H_2/H_1 \ll 1$. In this section, we assume that $R_\alpha = \mathcal{O}(1)$ and, tacitly, that Σ_1 is constant and $z_2 < H_2$. Note that, essentially, we have introduced two mean potentials in (19)

$$\bar{M}_1 = \theta_1\,(\Sigma_1)^\kappa - Z_0 \quad \text{and} \qquad \bar{M}_2 = \theta_2\,(\Sigma_1)^\kappa/\delta_a. \tag{20}$$

The following two remarks can be made about the scaling and the result (19). (a) The dimensionless potential $M_1 = \varepsilon^2\,M_1' +$ *a constant* such that $\nabla M_1 = \varepsilon^2\,\nabla M_1'$, which is used in the manipulations leading to (18)–(19). (b) Likewise $M_2 = F_2^2\,M_2' +$ *a constant* such that $\nabla M_2 = F_2^2\,\nabla M_2'$. Since $F_2^2 = \varepsilon^2/\delta_a = \varepsilon^2\,H_1/H_2$, M_2 could have been scaled with $g\,H_1$ after all, although it remains more clear to scale h_2 with H_2. The present scaling emphasizes, however, that F_2 and hence U_2 are defined by H_1 and H_2, which defines ε, and δ_a. The latter two parameters, ε and δ_a, both go to zero asymptotically. Finally, the system (18) has obtained a form, (A.16), generic in singular perturbation theory of systems with two times scales. Here it is written on the slow time scale, while t/ε is the fast time scale.

(i) *Observational basis scaling*

Our estimates are based on zonally averaged climatological seasonal radiosonde data displayed in Birner (2006), where potential temperature and horizontal wind speed are displayed as function of height and latitude. On request, Dr. Birner extracted vertical profiles of potential temperature and pressure at about 57.25^oN versus height, see Fig. 2. It seems reasonable to take $Z_2 = 10.63$km for the tropopause height and, say, $Z_1 = 16.63$km and $Z_0 = 34.63$km. Hence, $H_1 = 6$km and $H_1 = 18$km. Estimates for the horizontal velocities are $U_1^{\rm obs} \approx 2$m/s and $U_2^{\rm obs} \approx 14$m/s (from Fig. 7 of Birner, 2006). From Fig. 2, average values of the potential temperature are found to be approximately $\theta_2 = 381$K and $\theta_1^{\rm obs} = 672$K. Likewise, pressures observed and deduced at these heights are $p_2 = 241.74$mb, $p_1^{\rm obs} = 97$mb, and $p_0 = 6.185$mb. In our scaling, F_1, F_2, ε, θ_1 and p_1 follow, for example, after choosing $\theta_2, H_1, H_2, p_2, p_0, U_1$ and U_2. Further constants used are $g = 9.81$m/s, $c_p = 1004.6$J/(kg K) and $R = 287.04$J/(kg K) such that $\kappa = 2/7$. We obtain $F_1 = 0.0048$, $F_2 = 0.0577$, $\varepsilon = 0.1429$, and $\theta_1 = 629$K and $p_1 = 97$mb. This pressure value compares well with the observed value, while the calculated and observed potential temperature differ somewhat because the observed buoyancy frequency (and temperature) is roughly constant and not the entropy as in our layer model. Nevertheless, the data provide an observational basis for the chosen scaling.

(*c*) *Constraints*

Asymptotic analysis of the upper layer yields at leading order in ε, that is at $\mathcal{O}(1/\varepsilon)$ in (18), two constraints

$$\phi_1 = M_1'|_{\varepsilon=0} = 0 \qquad \text{and} \qquad D_1 = \boldsymbol{\nabla}\boldsymbol{\cdot}(\Sigma_1\,\mathbf{v}_1) = 0. \tag{21}$$

We introduce a fast time scale $\tau = t/\varepsilon$ and evaluate (18) at leading order; that is, we truncate the system (18) and (19) at the fast time scale by taking the limit $\varepsilon \to 0$ (after multiplication by ε). The following linear wave equations then appear after some manipulation:

$$\begin{aligned} \frac{\partial \sigma_1'}{\partial \tau} + D_1 = 0, \qquad & \frac{\partial D_1}{\partial \tau} = -\boldsymbol{\nabla}\cdot(\Sigma_1\,\boldsymbol{\nabla} M_1'|_{\varepsilon=0}), \\ \frac{\partial \omega_1}{\partial \tau} = 0, \qquad & \frac{\partial \sigma_2}{\partial \tau} = 0, \qquad \frac{\partial \mathbf{v}_2}{\partial \tau} = 0 \end{aligned} \tag{22}$$

with vorticity $\omega_1 = \boldsymbol{\nabla}^{\perp}\cdot\mathbf{v}_1$ and leading order potentials

$$\begin{aligned} M_1'|_{\varepsilon=0} &= \kappa\,(\Sigma_1)^{\kappa-1}\big(\theta_1\,\sigma_1' + \theta_2\,(\sigma_1' + \sigma_2)\big) + z_2 \quad \text{and} \\ M_2'|_{\varepsilon=0} &= \kappa\,\theta_2\,(\Sigma_1)^{\kappa-1}(\sigma_1' + \sigma_2) + z_2. \end{aligned} \tag{23}$$

The system (22) and (23) shows that the fast variables σ_1' and D_1 oscillate rapidly, while the slow variables ω_1, σ_2 and $\mathbf{v}_2$ vary on the slow time scale. The introduction of fast and slow variables is based on the distinction between high-frequency and low-frequency waves in linearized wave equations (Van Kampen, 1985). We will next consider the reduced, Hamiltonian dynamics on the "slow" manifold defined by these two constraints (21).

(*d*) *Constrained Hamiltonian formulation of $1\frac{1}{2}$-layer equations*

A dimensional Hamiltonian formulation of the two-layer system is introduced to derive the formulation for the $1\frac{1}{2}$-layer system. It consists of the evolution

$$\frac{\mathrm{d}\mathcal{F}}{\mathrm{d}t} = \{\mathcal{F}, \mathcal{H}\} \tag{24}$$

with the shallow-layer Poisson bracket in both layers ($\alpha = 1, 2$)

$$\{\mathcal{F}, \mathcal{G}\} = \sum_{\alpha=1}^{2} \iint q_\alpha \, \frac{\delta \mathcal{F}}{\delta \mathbf{v}_\alpha}^{\perp} \cdot \frac{\delta \mathcal{G}}{\delta \mathbf{v}_\alpha} - \frac{\delta \mathcal{F}}{\delta \sigma_\alpha} \boldsymbol{\nabla} \cdot \frac{\delta \mathcal{G}}{\delta \mathbf{v}_\alpha} + \frac{\delta \mathcal{G}}{\delta \sigma_\alpha} \boldsymbol{\nabla} \cdot \frac{\delta \mathcal{F}}{\delta \mathbf{v}_\alpha} \; \mathrm{d}x \, \mathrm{d}y \tag{25}$$

for arbitrary functionals $\mathcal{F}$ and $\mathcal{G}$ of $\{\mathbf{v}_\alpha, \sigma_\alpha\}$, a Hamiltonian

$$\begin{aligned} \mathcal{H} = \iint \sum_{\alpha=1}^{2} \big(\frac{1}{2}\, \sigma_\alpha \, |\mathbf{v}_\alpha|^2 + g \, \sigma_\alpha \, z_2\big) + \frac{p_r \, c_p \, \theta_2}{g \, (\kappa+1)} \, (\eta_2^{\kappa+1} - \eta_1^{\kappa+1}) + \\ \frac{p_r \, c_p \, \theta_1}{g \, (\kappa+1)} \, \eta_1^{\kappa+1} - \sigma_1 \, (c_p \, \theta_1 \, \eta_0^{\kappa} + g \, Z_0) \; \mathrm{d}x \, \mathrm{d}y, \end{aligned} \tag{26}$$

and the potential vorticity q_α in each layer α

$$q_\alpha = (\mathsf{f} + \boldsymbol{\nabla}^{\perp} \cdot \mathbf{v}_\alpha)/\sigma_\alpha \tag{27}$$

appearing in (25). The bracket (25) follows from the bracket in Bokhove and Oliver (2007) and equals the bracket in Bokhove (2002a). The Hamiltonian follows either directly from the Eulerian or parcel Eulerian-Lagrangian momentum equations or from the Hamiltonian of the three-dimensional Euler equations by neglecting the vertical velocity relative to the horizontal velocities, by using hydrostatic balance and the ideal gas law, and integration in the vertical over each isentropic layer (cf., Bokhove, 2002a). In the latter integration, the horizontal velocity is assumed to be independent of the depth in each layer and the last term in (26) is then absent. This last term, linear in σ_1, can arise without problem because any multiple of the mass $\iint \sigma_1 \, \mathrm{d}x \, \mathrm{d}y$ in the upper layer is a Casimir invariant and can be added to the Hamiltonian without changing the dynamics (cf., Shepherd, 1990). After taking the variation, it amounts to adding a constant to the Montgomery potential, which is always allowed. This addition further ensures that $M_1 = g\,(z_0 - Z_0)$, a useful simplification as we have seen. The functional derivatives of the Hamiltonian (26) are

$$\frac{\delta \mathcal{H}}{\delta \mathbf{v}_\alpha} = \sigma_\alpha \, \mathbf{v}_\alpha \qquad \text{and} \qquad \frac{\delta \mathcal{H}}{\delta \sigma_\alpha} = |\mathbf{v}_\alpha|^2/2 + M_\alpha, \tag{28}$$

with which it can be verified that (24) yields the equations of motion (1) in both layers when we choose the *functionals* $\mathcal{F} = \boldsymbol{v}_\alpha(\boldsymbol{x}, t) = \iint \delta(\boldsymbol{x} - \boldsymbol{x}') \, \boldsymbol{v}_\alpha(\boldsymbol{x}', t) \, \mathrm{d}x' \, dy'$ and $\mathcal{F} = \sigma_\alpha(\boldsymbol{x}, t) = \iint \delta(\boldsymbol{x} - \boldsymbol{x}') \, \sigma_\alpha(\boldsymbol{x}', t) \, \mathrm{d}x' \, \mathrm{d}y'$, respectively (see, *e.g.*, Shepherd, 1990, for an introduction on Hamiltonian fluid dynamics). The second part of (28) follows from (26) after some calculation by using the definitions of the Montgomery potentials in (2) and (3), $\eta_1 = p_1/p_r$, $\eta_2 = p_2/p_r$, and the pseudo-densities (15) in (1).

The formulation (24)–(26) is Hamiltonian as it satisfies the following properties (Bokhove and Oliver, 2007). The bracket $\{\mathcal{F}, \mathcal{G}\}$ is antisymmetric $\{\mathcal{F}, \mathcal{G}\} = -\{\mathcal{G}, \mathcal{F}\}$, and satisfies the Jacobi identity

$$\{\mathcal{F}, \{\mathcal{G}, \mathcal{K}\}\} + \{\mathcal{G}, \{\mathcal{K}, \mathcal{F}\}\} + \{\mathcal{K}, \{\mathcal{F}, \mathcal{G}\}\} = 0 \tag{29}$$

for arbitrary functional $\mathcal{F}, \mathcal{G}$ and $\mathcal{K}$. In the verification of these properties boundary conditions are required such as periodic boundaries; quiescence and constancy at infinity where σ_α is constant and $\mathbf{v}_\alpha = 0$; slip flow along walls, such that $\mathbf{v}_\alpha \cdot \hat{\mathbf{n}} = 0$ with $\hat{\mathbf{n}}$ the outward-pointing normal to the wall; or, combinations of these boundary conditions. Furthermore, in these verifications the functional derivatives have to be restricted to satisfy corresponding boundary conditions.

The scaled Hamiltonian dynamics is as follows

$$
\begin{aligned}
\frac{\mathrm{d}\mathcal{F}}{\mathrm{d}t} = \{\mathcal{F}, \mathcal{H}\} = \iint & \varepsilon\, q_1 \frac{\delta \mathcal{F}}{\delta \mathbf{v}_1}^{\perp} \cdot \frac{\delta \mathcal{H}}{\delta \mathbf{v}_1} - \frac{1}{\varepsilon} \frac{\delta \mathcal{F}}{\delta \sigma_1'} \boldsymbol{\nabla} \cdot \frac{\delta \mathcal{H}}{\delta \mathbf{v}_1} + \frac{1}{\varepsilon} \frac{\delta \mathcal{H}}{\delta \sigma_1'} \boldsymbol{\nabla} \cdot \frac{\delta \mathcal{F}}{\delta \mathbf{v}_1} \\
& + q_2 \frac{\delta \mathcal{F}}{\delta \mathbf{v}_2}^{\perp} \cdot \frac{\delta \mathcal{H}}{\delta \mathbf{v}_2} - \frac{\delta \mathcal{F}}{\delta \sigma_2} \boldsymbol{\nabla} \cdot \frac{\delta \mathcal{H}}{\delta \mathbf{v}_2} + \frac{\delta \mathcal{H}}{\delta \sigma_2} \boldsymbol{\nabla} \cdot \frac{\delta \mathcal{F}}{\delta \mathbf{v}_2}\ \mathrm{d}x\, \mathrm{d}y
\end{aligned} \tag{30}
$$

with potential vorticities

$$
q_1 = (1/R_1 + \omega_1)/(\Sigma_1 + \varepsilon^2\, \sigma_1') \qquad \text{and} \qquad q_2 = (1/R_2 + \boldsymbol{\nabla}^{\perp} \cdot \mathbf{v}_1)/\sigma_2, \tag{31}
$$

and modified Hamiltonian (cf. (A.15))

$$
\begin{aligned}
\mathcal{H} = \iint & \frac{1}{2} (\Sigma_1 + \varepsilon^2\, \sigma_1') \, |\mathbf{v}_1|^2 + \sigma_1'\, z_2 + \frac{1}{2} \sigma_2\, |\mathbf{v}_2|^2 + \sigma_2\, z_2 + \\
& \frac{1}{\varepsilon^4} \frac{\theta_2}{\kappa+1} \left((\Sigma_1 + \varepsilon^2\, \sigma_1' + \varepsilon^2\, \sigma_2)^{\kappa+1} - (\Sigma_1 + \varepsilon^2\, \sigma_1')^{\kappa+1} \right) - \frac{\theta_1}{\kappa+1} \frac{1}{\varepsilon^4} (\Sigma_1)^{\kappa+1} + \\
& \frac{\theta_1}{\varepsilon^4} \frac{1}{\kappa+1} (\Sigma_1 + \varepsilon^2\, \sigma_1')^{\kappa+1} - \frac{\left(\theta_1\, \sigma_1' + \theta_2\, \sigma_2\right)}{\varepsilon^2} (\Sigma_1)^{\kappa}\ \mathrm{d}x\, \mathrm{d}y.
\end{aligned} \tag{32}
$$

The additional terms, constant and linear in σ_1' and σ_2, are added to formally obtain a Hamiltonian non-singular as $\varepsilon \to 0$. These extra terms arise because mass is globally conserved in each layer and can be introduced formally by adding constants and mass Casimirs $\mathcal{C}_1 = \lambda_1 \iint (\Sigma_1 + \varepsilon^2\, \sigma_1')\, \mathrm{d}x\, \mathrm{d}y$ and $\mathcal{C}_2 = \lambda_2 \iint \varepsilon^2\, \sigma_2\, \mathrm{d}x\, \mathrm{d}y$ to the original, scaled Hamiltonian $\tilde{\mathcal{H}}$ (not shown) for suitable choices of λ_1 and λ_2 such that the singular terms constant and linear in σ_1' and σ_2 are eliminated. These above Casimirs are conserved since $\mathrm{d}\mathcal{C}_1/\mathrm{d}t = \{\mathcal{C}_1, \tilde{\mathcal{H}}\} = 0$ and $\mathrm{d}\mathcal{C}_2/\mathrm{d}t = \{\mathcal{C}_2, \tilde{\mathcal{H}}\} = 0$. The above expression is related but not quite equivalent to the available potential energy (Shepherd, 1993). Here it suffices to note that it yields the proper equations of motion. Akin to the dimensional case, the variational derivatives of (32) are readily calculated to be

$$
\begin{aligned}
& \frac{\delta \mathcal{H}}{\delta \sigma_1'} = \varepsilon^2\, |\mathbf{v}_1|^2/2 + M_1', \quad \frac{\delta \mathcal{H}}{\delta \sigma_2} = |\mathbf{v}_2|^2/2 + M_2', \\
& \frac{\delta \mathcal{H}}{\delta \mathbf{v}_1} = (\Sigma_1 + \varepsilon^2\, \sigma_1')\, \mathbf{v}_1 \quad \text{and} \quad \frac{\delta \mathcal{H}}{\delta \mathbf{v}_2} = \sigma_2\, \mathbf{v}_2.
\end{aligned} \tag{33}
$$

Substitution of (33) into (30) yields the scaled equations of motion (18) with (19).

Henceforth in this section, we use for simplicity and without further notice periodic boundary conditions or quiescence and constancy at infinity. Given the constraints $\phi_1' = M_1' = 0$ and $D_1 = \boldsymbol{\nabla}\cdot(\Sigma_1\, \mathbf{v}_1) = 0$, we can transform the Poisson bracket (30) in terms of the six variables $(\mathbf{v}_\alpha, \sigma_1', \sigma_2)$ to the variables $(\phi_1', D_1, \omega_1, \mathbf{v}_2, \sigma_2)$ with $\omega_1 = \boldsymbol{\nabla}^{\perp} \cdot \mathbf{v}_1$ the vorticity in the top layer. The functional derivatives with respect to the former variables relate to ones in terms of the latter variables as follows

$$\begin{aligned}
&\frac{\delta\mathcal{F}}{\delta\mathbf{v}_1}\Big|_{\sigma_1'} = -\big(\boldsymbol{\nabla}^{\perp}\frac{\delta\mathcal{F}}{\delta\omega_1} + \Sigma_1\,\boldsymbol{\nabla}\frac{\delta\mathcal{F}}{\delta D_1}\big), \quad \frac{\delta\mathcal{F}}{\delta\mathbf{v}_2}\Big|_{\sigma_1'} = \frac{\delta\mathcal{F}}{\delta\mathbf{v}_2}\Big|_{\phi_1}\\
&\frac{\delta\mathcal{F}}{\delta\sigma_1'}\Big|_{\mathbf{v}_1} = \frac{\partial M_1'}{\partial\sigma_1'}\,\frac{\delta\mathcal{F}}{\delta\phi_1}, \quad \frac{\delta\mathcal{F}}{\delta\sigma_2}\Big|_{\mathbf{v}_1,\sigma_1'} = \frac{\delta\mathcal{F}}{\delta\sigma_2}\Big|_{\phi_1} + \frac{\partial M_1'}{\partial\sigma_2}\,\frac{\delta\mathcal{F}}{\delta\phi_1}.
\end{aligned} \tag{34}$$

After substitution of (34) into (30) and rearrangement, we find (cf. the generic form (A.16) for finite-dimensional systems)

$$\begin{aligned}
\frac{\mathrm{d}\mathcal{F}}{\mathrm{d}t} = \{\mathcal{F},\mathcal{H}\} = \iint &\varepsilon\, q_1\, J\Big(\frac{\delta\mathcal{F}}{\delta\omega_1},\frac{\delta\mathcal{H}}{\delta\omega_1}\Big) + \varepsilon\,(\Sigma_1)^2\, q_1\, J\Big(\frac{\delta\mathcal{F}}{\delta D_1},\frac{\delta\mathcal{H}}{\delta D_1}\Big) +\\
&\varepsilon\,\Sigma_1\, q_1 \Big[\Big(\boldsymbol{\nabla}\frac{\delta\mathcal{H}}{\delta\omega_1}\Big)\cdot\boldsymbol{\nabla}\frac{\delta\mathcal{F}}{\delta D_1} - \Big(\boldsymbol{\nabla}\frac{\delta\mathcal{F}}{\delta\omega_1}\Big)\cdot\boldsymbol{\nabla}\frac{\delta\mathcal{H}}{\delta D_1}\Big] +\\
&\frac{1}{\varepsilon}\,\frac{\partial M_1'}{\partial\sigma_1'}\Big[\frac{\delta\mathcal{F}}{\delta\phi_1}\,\boldsymbol{\nabla}\cdot\Big(\Sigma_1\boldsymbol{\nabla}\frac{\delta\mathcal{H}}{\delta D_1}\Big) - \frac{\delta\mathcal{H}}{\delta\phi_1}\,\boldsymbol{\nabla}\cdot\Big(\Sigma_1\boldsymbol{\nabla}\frac{\delta\mathcal{F}}{\delta D_1}\Big)\Big] +\\
&q_2\,\frac{\delta\mathcal{F}}{\delta\mathbf{v}_2}^{\perp}\cdot\frac{\delta\mathcal{H}}{\delta\mathbf{v}_2} - \Big(\frac{\delta\mathcal{F}}{\delta\sigma_2} + \frac{\partial M_1'}{\partial\sigma_2}\,\frac{\delta\mathcal{F}}{\delta\phi_1}\Big)\boldsymbol{\nabla}\cdot\frac{\delta\mathcal{H}}{\delta\mathbf{v}_2} +\\
&\Big(\frac{\delta\mathcal{H}}{\delta\sigma_2} + \frac{\partial M_1'}{\partial\sigma_2}\,\frac{\delta\mathcal{H}}{\delta\phi_1'}\Big)\boldsymbol{\nabla}\cdot\frac{\delta\mathcal{F}}{\delta\mathbf{v}_2}\;\mathrm{d}x\,\mathrm{d}y
\end{aligned} \tag{35}$$

with $J(a,b) := (\partial_x a)(\partial_y b) - (\partial_x b)(\partial_y a)$ the Jacobian. Note the correspondence of the Hamiltonian dynamics (35) with the dynamics of the generic finite-dimensional Hamiltonian form (A.16) with bracket (A.14) in Appendix A. From (31), it follows that q_α is $\mathcal{O}(1)$.

From (33), (34) and (35) we derive

$$\begin{aligned}
\frac{\partial\phi_1(x,y,t)}{\partial t} &= \{\phi_1(x,y,t),\mathcal{H}\}\\
&= \frac{1}{\varepsilon}\,\frac{\partial M_1'}{\partial\sigma_1'}\,\boldsymbol{\nabla}\cdot\Big(\Sigma_1\boldsymbol{\nabla}\frac{\delta\mathcal{H}}{\delta D_1}\Big) - \frac{\partial M_1'}{\partial\sigma_2}\,\boldsymbol{\nabla}\cdot\frac{\delta\mathcal{H}}{\delta\mathbf{v}_2},\\
\frac{\partial D_1(x,y,t)}{\partial t} &= \{D_1(x,y,t),\mathcal{H}\} = -\varepsilon\,\boldsymbol{\nabla}\cdot\Big(\Sigma_1\, q_1\,\boldsymbol{\nabla}\frac{\delta\mathcal{H}}{\delta\omega_1}\Big)\\
&\quad + \varepsilon\, J\Big(\frac{\delta\mathcal{H}}{\delta D_1},\Sigma_1^2\, q_1\Big) - \frac{1}{\varepsilon}\,\boldsymbol{\nabla}\cdot\Big(\Sigma_1\boldsymbol{\nabla}\Big(\frac{\partial M_1'}{\partial\sigma_1'}\,\frac{\delta\mathcal{H}}{\delta\phi_1}\Big)\Big),\\
\frac{\partial\omega_1(x,y,t)}{\partial t} &= -\varepsilon\, J(q_1,\frac{\delta\mathcal{H}}{\delta\omega_1}) + \varepsilon\boldsymbol{\nabla}\cdot\big(\Sigma_1\, q_1\,\boldsymbol{\nabla}\frac{\delta\mathcal{H}}{\delta D_1}\big),\\
\frac{\partial\mathbf{v}_2(x,y,t)}{\partial t} &= -q_2\,\boldsymbol{\nabla}^{\perp}\frac{\delta\mathcal{H}}{\delta\mathbf{v}_2} - \boldsymbol{\nabla}\Big(\frac{\delta\mathcal{H}}{\delta\sigma_2} + \frac{\partial M_1'}{\partial\sigma_2}\,\frac{\delta\mathcal{H}}{\delta\phi_1}\Big),\\
\frac{\partial\sigma_2(x,y,t)}{\partial t} &= -\boldsymbol{\nabla}\frac{\delta\mathcal{H}}{\delta\mathbf{v}_2}.
\end{aligned} \tag{36}$$

At leading order in ε the variational derivative of the Hamiltonian is

$$\begin{aligned}
\delta\mathcal{H} = \iint &-\chi\,\delta D_1 - \Psi\,\delta\omega_1 + M_1'|_{\varepsilon=0}\,\delta\sigma_1' + \sigma_2\,\mathbf{v}_2\;\cdot\delta\mathbf{v}_2 +\\
&(\frac{1}{2}\,|\mathbf{v}_2|^2 + M_2'|_{\varepsilon=0})\,\delta\sigma_2\;\mathrm{d}x\,\mathrm{d}y
\end{aligned} \tag{37}$$

in which we have used $\Sigma_1\,\mathbf{v}_1 = \Sigma_1\,\boldsymbol{\nabla}\chi + \boldsymbol{\nabla}^\perp\Psi$ with velocity potential χ and (transport) streamfunction Ψ. Therefore, using (34) one finds

$$\frac{\delta\mathcal{H}}{\delta D_1}\Big|_{\varepsilon=0} = -\chi \qquad \text{and} \qquad \frac{\delta\mathcal{H}}{\delta\sigma_1'}\Big|_{\varepsilon=0} = M_1'|_{\varepsilon=0}. \tag{38}$$

Evaluation of (36) at leading order in ε gives

$$\varepsilon\,\frac{\partial\phi_1}{\partial t} \propto D_1 = 0 \qquad \text{and} \qquad \varepsilon\,\frac{\partial D_1}{\partial t} \propto \boldsymbol{\nabla}\cdot\left(\Sigma_1\boldsymbol{\nabla}M_1'|_{\varepsilon=0}\right) = 0 \tag{39}$$

giving the constraints (21) as a solution, which shows consistency at leading order. Hence, at leading order in ε we take $\delta\mathcal{H}/\delta\phi_1|_{\varepsilon=0} = \delta\mathcal{H}/\delta D_1|_{\varepsilon=0} = 0$ and from (36) we find the balanced dynamics on the slow manifold; that is, we truncate the dynamics to the leading order terms in ε. First, the vorticity dynamics in the upper layer is frozen in time

$$\frac{\partial\omega_1}{\partial t} = 0, \tag{40}$$

which we further simplify by initializing $\omega_1(x,y,0) = 0$. Together with $D_1 = 0$, this explains why it is asymptotically sound to take $\mathbf{v}_1 = 0$ at leading order, as we discussed in the introduction. Second, the balanced dynamics in the lower layer then becomes

$$\frac{\partial\mathbf{v}_2}{\partial t} = -q_2\,\boldsymbol{\nabla}^\perp\frac{\delta\mathcal{H}_0}{\delta\mathbf{v}_2} - \boldsymbol{\nabla}\frac{\delta\mathcal{H}_0}{\delta\sigma_2}, \quad \text{and} \quad \frac{\partial\sigma_2}{\partial t} = -\boldsymbol{\nabla}\cdot\frac{\delta\mathcal{H}_0}{\delta\mathbf{v}_2} \tag{41}$$

with $\mathcal{H}_0$ arising from (30) as the leading-order Hamiltonian on the constrained manifold:

$$\begin{aligned}\mathcal{H}_0 = \iint\, &\frac{1}{2}\,\sigma_2\,|\mathbf{v}_2|^2 + (\sigma_1' + \sigma_2)\,z_2 \\ &+ \frac{1}{2}\,\theta_2\,\kappa\,\Sigma_1^{\kappa-1}\left((\sigma_1'+\sigma_2)^2 - {\sigma_1'}^2\right) + \frac{1}{2}\,\theta_1\,\kappa\,\Sigma_1^{\kappa-1}\,{\sigma_1'}^2\;\mathrm{d}x\,\mathrm{d}y.\end{aligned} \tag{42}$$

Variation of (42) gives

$$\begin{aligned}\delta\mathcal{H}_0 &= \iint \sigma_2\,\mathbf{v}_2\cdot\delta\mathbf{v}_2 + \big(\frac{1}{2}\,|\mathbf{v}_2|^2 + M_2|_{\varepsilon=0}\big)\,\delta\sigma_2 + M_1'|_{\varepsilon=0}\,\delta\sigma_1'\;\mathrm{d}x\,\mathrm{d}y \\ &= \iint \sigma_2\,\mathbf{v}_2\cdot\delta\mathbf{v}_2 + \big(\frac{1}{2}\,|\mathbf{v}_2|^2 + M_2|_{\varepsilon=0}\big)\,\delta\sigma_2\end{aligned} \tag{43}$$

using the constraint $M_1'|_{\varepsilon=0} = 0$, cf. (21) and (23). Alternatively, by including higher order terms in ε and using the (higher-order) constraint $M_1 = 0$, but only in the Hamiltonian, we can use the original Hamiltonian (32) on the constrained manifold $\mathbf{v}_1 = 0$ (by initializing $\omega_1(x,y,0) = 0$) and $M_1 = 0$. The generalized Poisson bracket is then truncated to leading order on the (leading-order) constrained manifold, but the Hamiltonian $\mathcal{H}_{\mathbf{v}_1=0,M_1=0}$ is chosen and includes higher-order terms in ε. When we truncate this higher-order Hamiltonian one finds again $\mathcal{H}_0$, of course, as $\mathcal{H}_{\mathbf{v}_1=0,M_1=0} \rightarrow_{\varepsilon\to0} \mathcal{H}_0$ with $M_1'|_{\varepsilon=0} = 0$. This reduced Hamiltonian is chosen because it simply amounts to setting $\mathbf{v}_1 = 0$ and $z_0 = Z_0$ to get the rigid-lid approximation $M_1 = 0$ in the Hamiltonian, see below in § 2d(ii), which then provides a clear physical procedure for our approximation, as given in Fig. 1.

The dynamics on the constrained manifold is governed by the slow variables $\{\omega_1 = 0, \mathbf{v}_2, \sigma_2\}$, since the dynamics of the fast variables $\{D_1, \sigma_1'\}$ or $\{D_1, \phi_1\}$ associated with the gravity waves in layer one is absent at leading order. Restricting or truncating the transformed bracket (35) to the constrained manifold and keeping all leading-order terms in ε, the following (dimensional and dimensionless) constrained dynamics emerges

$$\frac{\mathrm{d}\mathcal{F}_c}{\mathrm{d}t} = \{\mathcal{F}_c, \mathcal{H}_c\}_c = \iint q_2 \, \frac{\delta \mathcal{F}_c}{\delta \mathbf{v}_2}^{\perp} \cdot \frac{\delta \mathcal{H}_c}{\delta \mathbf{v}_2} - \frac{\delta \mathcal{F}_c}{\delta \sigma_2} \boldsymbol{\nabla} \cdot \frac{\delta \mathcal{H}_c}{\delta \mathbf{v}_2} + \frac{\delta \mathcal{H}_c}{\delta \sigma_2} \boldsymbol{\nabla} \cdot \frac{\delta \mathcal{F}_c}{\delta \mathbf{v}_2} \, \mathrm{d}x \, \mathrm{d}y. \tag{44}$$

with the constrained Hamiltonian either $\mathcal{H}_c = \mathcal{H}_0$ (with $M_1'|_{\varepsilon=0} = 0$) or $\mathcal{H}_c = \mathcal{H}_{\mathbf{v}_1=0, M_1=0}$. We emphasize that $\mathcal{F}_c$ and $\mathcal{H}_c$ are functionals of the slow variables $\mathbf{v}_2$ and σ_2 only.

(i) *The Jacobi identity*

The Jacobi identity is satisfied by the bracket (44) since it consists of the original bracket in (30) for the second, lower layer which was originally already separate from the bracket for the first, upper layer. The preservation of the Jacobi identity for the leading-order reduced bracket (44) was particularly simple in the asymptotic analysis presented. In general, the leading-order reduced bracket resulting from a singular perturbation approach is more complicated. The theory presented in Appendix A(b) for finite-dimensional Hamiltonian systems then provides a handle for dealing with the Jacobi identity in such more complex infinite-dimensional cases. Application of this theory would provide another proof of the Jacobi identity of the bracket (44), in a particular extension to the current continuum case.

(ii) *Dimensional dynamics*

Finally, the dynamics on the constrained manifold is given by (24) for $\mathcal{F} = \mathcal{F}_c$ and $\mathcal{H} = \mathcal{H}_c$ with (44) and dimensional constrained Hamiltonian

$$\begin{aligned} \mathcal{H}_c = \iint & \frac{1}{2} \, \sigma_2 \, |\mathbf{v}_2|^2 + g \, (\sigma_1 + \sigma_2) \, z_2 + \\ & \frac{c_p \, p_r \, \theta_2}{g \, (\kappa + 1)} \, (\eta_2^{\kappa+1} - \eta_1^{\kappa+1}) + \frac{c_p \, p_r \, \theta_1}{g \, (\kappa + 1)} \, \eta_1^{\kappa+1} - \sigma_1 \, (c_p \, \theta_1 \, \eta_0^{\kappa} + g \, Z_0) \, \mathrm{d}x \, \mathrm{d}y \end{aligned} \tag{45}$$

with $\sigma_2 = (p_2 - p_1)/g$, $\sigma_1 = p_1/g$, and the constraint $M_1 = 0$ (i.e. $z_0 = Z_0$) relating $\eta_1 = p_1/p_r$ to $\eta_2 = p_2/p_r$, that is,

$$M_1 = c_p \, \theta_2 \, \eta_2^{\kappa} + c_p \, (\theta_1 - \theta_2) \, \eta_1^{\kappa} + g \, (z_2 - Z_0) = 0. \tag{46}$$

As argued earlier, instead of using the constrained Hamiltonian truncated to leading order in ε we use the original Hamiltonian reduced to the constraint or "rigid-lid" manifold $M_1 = 0$ (and $\mathbf{v}_1 = 0$). Hence, we included higher-order terms in ε in the Hamiltonian, which does not hamper the leading-order accuracy since the constrained bracket (44) is leading order. The functional derivative of the potential and internal energy in (45) subject to constraint (46) is

$$\begin{aligned}\frac{\delta\mathcal{H}_{ci}}{\delta\sigma_2}\delta\,\sigma_2 &= \Big(z_2+\frac{c_p\,\theta_2}{g}\,\eta_2^\kappa\Big)\,\delta p_2+\Big(\frac{c_p\,(\theta_1-\theta_2)}{g}\,\eta_1^\kappa-Z_0\Big)\,\delta p_1\\ &= \Big(z_2+\frac{c_p\,\theta_2}{g}\,\eta_2^\kappa\Big)\,\delta p_2+\Big(\frac{c_p\,(\theta_1-\theta_2)}{g}\,\eta_1^\kappa-Z_0\Big)\,\frac{\partial p_1}{\partial p_2}\,\delta p_2\\ &= \Big(z_2+\frac{c_p\,\theta_2}{g}\,\eta_2^\kappa\Big)\,\Big(1-\frac{\partial p_1}{\partial p_2}\Big)\,\delta p_2=M_2\,\delta\sigma_2\end{aligned} \tag{47}$$

using the definition $g\,\sigma_2=p_2-p_1$ and with $\mathcal{H}_{ci}[\sigma_2]=\mathcal{H}_c[\mathbf{v}_2=0,\sigma_2]$ denoting the non-kinetic terms in the Hamiltonian. The equations of motion (1) for $\alpha=2$ thus stay the same with Montgomery potential (2), in which σ_1 is defined in terms of σ_2 and z_2 by $M_1=0$ via (3).

Recapitulating, we note that we have been able to construct the Hamiltonian formulation of the $1\frac{1}{2}$-layer model. *A posteriori*, we conclude that it is consistent to set $\mathbf{v}_1=0$, since in the first, upper layer we found $\omega_1=0$ by initializing $\omega_1(x,y,0)=0$ and $D_1=0$ in the small ε limit.

3. Hamiltonian formulation of nearly geostrophic balanced models

The Hamiltonian formulation of the $1\frac{1}{2}$-layer balanced model will be used as the starting point to derive nearly geostrophic Hamiltonian approximate or balanced models. Geostrophic balance is a balance between the Coriolis force and the gradient of the Montgomery potential

$$\mathsf{f}\,\mathbf{v}^\perp=-\boldsymbol{\nabla}M, \tag{48}$$

where we have dropped here and hereafter the layer subscripts when no confusion arises. Geostrophy results as the leading-order balance in an expansion of the variables in terms of a small Rossby number $R=U/(\mathsf{f}\,L)$, where U and L are velocity and length scales in the lower layer. We therefore start our approach with the bracket (44). *i.e.*, with the standard "shallow-water" bracket (Shepherd, 1990; Bokhove and Oliver, 2006)

$$\{\mathcal{F},\mathcal{G}\}_c=\iint q\,\frac{\delta\mathcal{F}}{\delta\mathbf{v}}^\perp\cdot\frac{\delta\mathcal{G}}{\delta\mathbf{v}}-\frac{\delta\mathcal{F}}{\delta\sigma}\boldsymbol{\nabla}\cdot\frac{\delta\mathcal{G}}{\delta\mathbf{v}}+\frac{\delta\mathcal{G}}{\delta\sigma}\boldsymbol{\nabla}\cdot\frac{\delta\mathcal{F}}{\delta\mathbf{v}}\,\mathrm{d}x\,\mathrm{d}y. \tag{49}$$

(*a*) *Velocity constraints and L1-dynamics*

Defining $\mathbf{v}=(u_1,u_2)$, we consider general velocity constraints $\tilde{\mathbf{v}}=(\tilde{u}_1,\tilde{u}_2)$ defined by

$$\tilde{u}_i=u_i-u_i^C=0 \tag{50}$$

for each component of the constraint horizontal velocity $\mathbf{v}^C$. The lowercase italic indices such as i,j run from 1 to 2. An example is, of course, the pair of geostrophic constraints

$$\tilde{u}_i=u_i+\epsilon_{ij}\,\frac{1}{\mathsf{f}}\,\partial_j M=0 \tag{51}$$

with $\partial_j=\partial/\partial x_j$, and ϵ_{ij} the permutation symbol such that $\epsilon_{11}=\epsilon_{22}=0$ and $\epsilon_{12}=-\epsilon_{21}=1$. The variation of the constraint velocity is

$$\delta u_i^C=\mathsf{D}^i\delta\sigma \tag{52}$$

with the Fréchet derivative D^i (*cf.*, Vanneste and Bokhove, 2002). We also require the adjoint of the Fréchet derivative, $\hat{\mathsf{D}}^i$, defined such that

$$\iint F\, \mathsf{D}^i G\, \mathrm{d}x\, \mathrm{d}y = \iint G\, \hat{\mathsf{D}}^i F\, \mathrm{d}x\, \mathrm{d}y \tag{53}$$

for arbitrary functions F and G. For the geostrophic constraint (51), we find

$$\mathsf{D}^i(\cdot) = -\frac{\epsilon_{ij}}{\mathsf{f}}\, \partial_j\Big(\frac{\partial M}{\partial \sigma}(\cdot)\Big) \qquad \text{and} \qquad \hat{\mathsf{D}}^i(\cdot) = \frac{\partial M}{\partial \sigma}\frac{\epsilon_{ij}}{\mathsf{f}}\, \partial_j(\cdot). \tag{54}$$

In defining these Fréchet derivatives, we must carefully analyze the boundary contributions: this analysis is left as an open problem. For periodic boundary conditions, quiescence at infinity, and when the thickness $h_2 \to 0$ such that $\delta\sigma \to 0$ at the boundary, the result (54) is valid.

Consider the transformation of functional derivatives from the set of variables $(\mathbf{v}, \sigma)$ to the set $(\tilde{\mathbf{v}}, \sigma)$

$$\frac{\delta \mathcal{F}}{\delta \sigma} = \frac{\delta \mathcal{F}}{\delta \sigma}\Big|_C - \hat{D}^i \frac{\delta \mathcal{F}}{\delta \tilde{u}_i} \qquad \text{and} \qquad \frac{\delta \mathcal{F}}{\delta u_i} = \frac{\delta \mathcal{F}}{\delta \tilde{u}_i}, \tag{55}$$

where $(\cdot)|_C$ denotes that we consider the functional derivative of σ with $\tilde{\mathbf{v}}$ held fixed. This will become a constrained derivative, if we realize that by constraining u_i to u_i^C we obtain

$$\begin{aligned} \delta \mathcal{F} &= \iint \Big(\frac{\delta \mathcal{F}}{\delta \sigma}\, \delta\sigma + \frac{\delta \mathcal{F}}{\delta u_i}\, \delta u_i^C\Big)\ \mathrm{d}x\, \mathrm{d}y \\ &= \iint \Big(\frac{\delta \mathcal{F}}{\delta \sigma} + \hat{D}^i \frac{\delta \mathcal{F}}{\delta u_i}\Big)\, \delta\sigma\ \ \mathrm{d}x\, \mathrm{d}y = \iint \frac{\delta \mathcal{F}}{\delta \sigma}\Big|_C\, \delta\sigma\, \mathrm{d}x\, \mathrm{d}y. \end{aligned} \tag{56}$$

In particular, additional boundary conditions may be required. For example, when we consider the geostrophic constraint (51) the variations become

$$\begin{aligned} \delta \mathcal{F} = \iint_D \Big[\frac{\delta \mathcal{F}}{\delta \sigma}\, \delta\sigma + \frac{\epsilon_{ij}}{f}\, \frac{\partial M}{\partial \sigma_2}\, \partial_i\Big(\frac{\delta \mathcal{F}}{\delta \tilde{u}_i}\Big)\, \delta\sigma + \frac{\delta \mathcal{F}}{\delta \tilde{u}_i}\, \delta u_i\Big]\, \mathrm{d}x\, \mathrm{d}y + \\ \int_{\partial D} \frac{\delta \mathcal{F}}{\delta \tilde{\mathbf{v}}} \cdot \hat{\mathbf{t}}\, \frac{\partial M}{\partial \sigma}\, \delta\sigma\, \mathrm{d}l, \end{aligned} \tag{57}$$

where $\mathrm{d}l$ is an infinitesimal line segment along, and $\hat{\mathbf{t}}$ a unit vector tangent to, the boundary. Hence, we set the tangential component of the (functional derivative of) ageostrophic velocity $\tilde{\mathbf{v}} = \mathbf{v} - \mathbf{v}^C$ to zero (*cf.*, Salmon, 1985) as additional boundary condition.

Substitution of (55) into the bracket (49) yields

$$\begin{aligned} \{\mathcal{F}, \mathcal{G}\}_c = \iint \Big\{ q\, \frac{\delta \mathcal{F}}{\delta \tilde{\mathbf{v}}}^{\perp} \cdot \frac{\delta \mathcal{G}}{\delta \tilde{\mathbf{v}}} - \frac{\delta \mathcal{F}}{\delta \sigma}\Big|_C \boldsymbol{\nabla} \cdot \frac{\delta \mathcal{G}}{\delta \tilde{\mathbf{v}}} + \frac{\delta \mathcal{G}}{\delta \sigma}\Big|_C \boldsymbol{\nabla} \cdot \frac{\delta \mathcal{F}}{\delta \tilde{\mathbf{v}}} \\ + \Big(\hat{D}^i \frac{\delta \mathcal{F}}{\delta \tilde{u}_i}\Big) \boldsymbol{\nabla} \cdot \frac{\delta \mathcal{G}}{\delta \tilde{\mathbf{v}}} - \Big(\hat{D}^i \frac{\delta \mathcal{G}}{\delta \tilde{u}_i}\Big) \boldsymbol{\nabla} \cdot \frac{\delta \mathcal{F}}{\delta \tilde{\mathbf{v}}} \Big\}\, \mathrm{d}x\, \mathrm{d}y. \end{aligned} \tag{58}$$

Note that only the second term in (58) remains on the constrained manifold, where conservation of mass holds

$$\frac{\partial \sigma}{\partial t} = -\boldsymbol{\nabla} \cdot \frac{\delta \mathcal{H}}{\delta \tilde{\mathbf{v}}}. \tag{59}$$

Consistency requires that the constraint is preserved in time

$$0 = \frac{\partial \tilde{u}_i}{\partial t} = q\, \epsilon_{ij} \frac{\delta \mathcal{H}}{\delta \tilde{u}_j} - \partial_i \frac{\delta \mathcal{H}}{\delta \sigma}\Big|_C + D^i \partial_j \frac{\delta \mathcal{H}}{\delta \tilde{u}_j} + \partial_i \Big(\hat{D}^j \frac{\delta \mathcal{H}}{\delta \tilde{u}_j} \Big), \tag{60}$$

in which $q = (\mathsf{f} + \epsilon_{ij}\, \partial_i u_j^C)/\sigma$ is the constrained potential vorticity. Hence,

$$\mathcal{L}^{ij} \frac{\delta \mathcal{H}}{\delta \tilde{u}_j} = \partial_i \frac{\delta \mathcal{H}}{\delta \sigma}\Big|_C, \tag{61}$$

where we have introduced the linear operator

$$\mathcal{L}^{ij} = q\, \epsilon_{ij} \frac{\delta \mathcal{H}}{\delta \tilde{u}_j} + D^i \partial_j \frac{\delta \mathcal{H}}{\delta \tilde{u}_j} + \partial_i \Big(\hat{D}^j \frac{\delta \mathcal{H}}{\delta \tilde{u}_j} \Big). \tag{62}$$

Finally, on the constrained manifold defined by the velocity constraints, we obtain Dirac's constrained dynamics and bracket (*cf.*, Vanneste and Bokhove, 2002) by substituting (61) into the second term in (58) or via a substitution into (59)

$$\frac{\mathrm{d}\mathcal{F}}{\mathrm{d}t} = \{\mathcal{F}, \mathcal{H}\}_C = \iint \partial_i \frac{\delta \mathcal{F}}{\delta \sigma}\Big|_C \mathcal{L}^{-ij}\, \partial_j \frac{\delta \mathcal{H}}{\delta \sigma}\Big|_C \mathrm{d}x\, \mathrm{d}y \tag{63}$$

after an integration by parts and after formally assuming that $\mathcal{L}$ is invertible. (In these last manipulations, we have assumed that boundary terms disappear. For periodic boundary conditions, for example, this is true.)

In contrast with previous derivations (Allen and Holm, 1996; Vanneste and Bokhove, 2002), we have not introduced any Lagrangian variables or Lagrange multipliers. In Appendix A, it is shown that the slaved Hamiltonian approach yields the Dirac bracket (Dirac, 1964) for general finite-dimensional systems. Dirac (1958) proved that this finite-dimensional Dirac bracket satisfies the Jacobi identity, while the antisymmetric property of this finite-dimensional Dirac bracket follows more directly. Since $\mathcal{L}^{ij}$ is antisymmetric under suitable boundary conditions and under the assumption that it is invertible, we note that the Dirac bracket in (63) is antisymmetric.

Balanced equations of motion appear when we use $\mathrm{d}\mathcal{F}_C/\mathrm{d}t = \{\mathcal{F}_C, \mathcal{H}_C\}_C$, (63) and the constrained Hamiltonian

$$\begin{aligned} \mathcal{H}_C = \iint & \frac{1}{2}\, \sigma\, |\mathbf{v}^C|^2 + g\, (\sigma + \sigma_1)\, z_2 + \frac{c_p\, p_r\, \theta_2}{g\, (\kappa + 1)}\, (\eta_2^{\kappa+1} - \eta_1^{\kappa+1}) + \\ & \frac{c_p\, p_r\, \theta_1}{g\, (\kappa+1)}\, \eta_1^{\kappa+1} - \sigma_1\, (c_p\, \theta_1\, \eta_1^{\kappa} + g\, Z_0)\, \mathrm{d}x\, \mathrm{d}y \end{aligned} \tag{64}$$

with $M_1 = 0$ [(46)] and $\sigma = \sigma_2$. In particular, we find L1-dynamics for a $1\frac{1}{2}$-layer isentropic model after we substitute the Fréchet derivatives (54) for the geostrophic constraint into (62) and (63), which then defines the balanced dynamics The only difference with the result in Vanneste and Bokhove (2002) is the Hamiltonian (64), which includes additional internal-energy terms.

4. Summary and concluding remarks

A two-layer stratospheric toy model with an isentropic lower and upper layer has been simplified systematically to a $1\frac{1}{2}$-layer model. Several small parameters emerged in the two-layer problem: Froude numbers F_2 and F_1 for the lower and upper layers, the ratio δ_a of the thicknesses of these layers, and the ratio ε of the wind speed in the upper layer over the wind speed in the lower layer (the latter is also the square root of the perturbation pseudo-density over the mean upper-layer pseudo-density). The final, scaled Hamiltonian system has the typical form of a two-time scale problem often encountered in (geophysical) fluid dynamics (Warn et al., 1995; Bokhove, 2002b; Appendix A). At leading order on the fast time scale, these systems have rapidly oscillating fast modes and slow modes with associated fast and slow variables.

The data from Birner (2006; see also Fig. 2) suggest that, in the stratosphere, the use of two isothermal layers (see Bokhove and Oliver, 2007) may be more realistic than the use of two isentropic layers. The Hamiltonian approaches presented apply directly to such an isothermal layer model. While isothermal layer models can be statically stable, whereas isentropic models are formally only neutrally stable, the former conservative models seem to require (implicit) forcing and dissipation to maintain the isothermal conditions.

Subsequently leading-order Hamiltonian perturbation theory was used to systematically derive the Hamiltonian formulation of the $1\frac{1}{2}$-layer equations, which represent the slow dynamics. Using a slaved Hamiltonian approach, the $1\frac{1}{2}$-layer equations were also considered in the limit of a small Rossby number, previously assumed to be of order one. With this slaved Hamiltonian approach the Hamiltonian L1-dynamics was (re)derived but for the novel $1\frac{1}{2}$-layer equation in a more succinct derivation than in Vanneste and Bokhove (2002).

The general character of the above two Hamiltonian perturbation approaches has been presented in Appendix A for finite-dimensional Hamiltonian systems. In this appendix, we considered finite-dimensional Hamiltonian systems with an even number of constraints which arise from a slaving approach as $\tilde{u} = u - U(s) = 0$ with u the slaved and s the slow variables. The ratio of slow to fast time scales was assumed to define a small parameter ε. At leading and higher order, an asymptotic or iterative approach then defines a sequence of constraints of the form $\tilde{u} = u - U_i(s) = 0$ with the index i representing the order of approximation. The consistency requirement of the constraint in time, $\mathrm{d}\tilde{u}/\mathrm{d}t = 0$, combined with the slow dynamics for s, then yields a slaved Hamiltonian dynamics on a constrained manifold with a Dirac bracket. Our derivation of the Dirac bracket is more concise than in Dirac (1958, 1964), because our slaving constraints are special, representing pairs of high-frequency waves.

The presented slaved Hamiltonian approach can be extended to infinite-dimensional systems on a case by case basis. In these systems, it can simplify the derivations of Hamiltonian reduced or balanced dynamics in Salmon (1985, 1988), Allen and Holm (1996), McIntyre and Roulstone (2002), and of the Dirac bracket in Vanneste and Bokhove (2002). Alternatively, it can provide other approximate Hamiltonian fluid systems, as the derivations in the text have illustrated. The leading-order Hamiltonian approach has been used to systematically derive the Hamiltonian formulation of the barotropic quasi-geostrophic equations and the incompressible three-dimensional (barotropic) equations in Bokhove (2002b).

Acknowledgements

O.B. gratefully acknowledges support by a fellowship from The Royal Netherlands Academy of Arts and Sciences. The Hamiltonian approach in Appendix

A originated in my Ph.D. dissertation (§4.4-4.5, University of Toronto, 1996). T.G.S. is supported by the Natural Sciences and Engineering Research Council of Canada. Appendix A benefitted from discussions with Dr. D. Wirosoetisno, during his stay at the University of Twente under a visitors' stipend from the Twente Institute of Mechanics. Finally, O.B. is indebted to Dr. W.T.M. Verkley for many discussions on the content of this research and pointing out an error in the original scaling. Unfortunately, our differences in style ultimately prohibited a joint publication.

Appendix A

Slaved Hamiltonian Dynamics —By O. Bokhove and T.G. Shepherd‡—

Let $\mathsf{z} = (s, u)$ be a state vector§ with $s \in \mathbf{R}^{p_s}$ and $u \in \mathbf{R}^q$, such that u and s are both vectors as well. Here, q is an even number and p_s may be either even or odd. Consider a (generalized) Hamiltonian structure, which is written as

$$\frac{\mathrm{d}\mathsf{z}}{\mathrm{d}t} = \{\mathsf{z}, H\} \tag{A.1}$$

for a Hamiltonian $H(\mathsf{z})$ and a (generalized) Poisson bracket $\{\cdot, \cdot\}$, and with time t. Both will be defined further below. The Poisson bracket $\{F, G\}$ of two functions $F(\mathsf{z})$ and $G(\mathsf{z})$ is antisymmetric, $\{F, G\} = -\{G, F\}$, and obeys the Jacobi identity

$$\{G_1, \{G_2, G_3\}\} + \{G_2, \{G_3, G_1\}\} + \{G_3, \{G_1, G_2\}\} = 0 \tag{A.2}$$

for arbitrary functions $G_1 = G_1(\mathsf{z})$, $G_2 = G_2(\mathsf{z})$ and $G_3 = G_3(\mathsf{z})$ of the state vector z (*e.g.*, Olver, 1986). Individual components will be denoted by superscripts, *i.e.*, z^i, s^i, and u^i, where indices run over the relevant ranges. More specifically, we write

$$\{F, G\} = (\partial F/\partial \mathsf{z}^i)\{\mathsf{z}^i, \mathsf{z}^j\}(\partial G/\partial \mathsf{z}^j), \tag{A.3}$$

where repeated indices are understood to be summed over the relevant ranges.

We denote $\partial_s := \partial/\partial s$ and $\partial_u := \partial/\partial u$. Again individual components will be denoted by superscripts: ∂_s^i and ∂_u^i, and $(\partial_u g)^{ij} := \partial g^j/\partial u^i$, etcetera. We consider generalized, finite-dimensional Hamiltonian systems subject to an even number of constraints $\tilde{u} = u - U(s) = 0$ between the variables u and variables s with function $U = U(s)$. The matrix of the generalized Poisson bracket of the constraints $\{\tilde{u}^i, \tilde{u}^j\}$ is assumed to be invertible. The outline of this Appendix is:

(a) In section (a), we show under the above assumption that the slaved Hamiltonian dynamics on the constrained manifold $\tilde{u} = 0$ follows directly from the equations of motion for s and $\tilde{u}$, subject to the consistency condition that the time evolution of the constraints is zero, *i.e.* $d\tilde{u}/dt = 0$. The resulting generalized Poisson bracket on the constrained manifold is the Dirac bracket.

(b) Finally, in section (b), we use that in many Hamiltonian systems the variables can be divided into slow variables s and fast variables f, instead of s and u. The ratio of slow to fast time scales then defines a small parameter ε. In these systems, the matrix of the bracket of constraints $\{\tilde{u}^i, \tilde{u}^j\}$, with now $\tilde{u} = f - U(s)$, is guaranteed to be invertible at leading order in ε. We show for this case that the slaved Hamiltonian approach can be simplified to a leading-order Hamiltonian slow dynamics on the approximated leading-order constrained manifold $f = 0$ emerging in the limit $\varepsilon \to 0$. The proof of the Jacobi identity is not entirely trivial for this leading order case.

‡ Department of Physics, University of Toronto, Toronto, Canada.

§ Notation in this appendix is autonomous and independent from the main text.

(a) Hamiltonian constrained dynamics

For the asymptotics we adopt the following notation: any function written in the form $F(\mathsf{z};\varepsilon)$ is understood to be of $\mathcal{O}(1)$, meaning that $\lim_{\varepsilon\to 0} F(\mathsf{z};\varepsilon)$ is finite. By $\mathcal{O}(\varepsilon^n)$ we mean $\varepsilon^n F(z;\varepsilon)$ for some $F(\mathsf{z};\varepsilon)$.

We consider constraints

$$\tilde{u} = u - U(s) = 0. \tag{A.4}$$

Otherwise stated, u is slaved to s (see Van Kampen, 1985). We suppose that these constraints are at least consistent to leading order in a suitably chosen small parameter ε arising in an appropriate scaling of the physical problem investigated. More particularly, we assume that the matrix of the generalized Poisson bracket of constraints, $\{\tilde{u}^i, \tilde{u}^j\}$, is invertible. This assumption will be motivated in §(*b*) using an asymptotic approach.

The variations of a function $F(\mathsf{z})$ in terms of variables $\mathsf{z} = (s, u)$ are related to the ones with variables $\mathsf{z} = (s, \tilde{u})$ as follows, *i.e.*, before we apply the constraints,

$$\delta F = \partial_s F\big|_C\, \delta s + \partial_{\tilde{u}} F\, \delta\tilde{u} = \big(\partial_s F\big|_C - \partial_{\tilde{u}} F\, \partial_s U\big)\, \delta s + \partial_{\tilde{u}} F\, \delta u, \tag{A.5}$$

where $(\cdot)|_C$ denotes that we consider derivatives of s with $\tilde{u}$ held fixed. Hence

$$\partial_s F = \partial_s F\big|_C - \partial_{\tilde{u}} F\, \partial_s U \qquad \text{and} \qquad \partial_u F = \partial_{\tilde{u}} F. \tag{A.6}$$

Consistency of the constraints requires that

$$\frac{\mathrm{d}\tilde{u}}{\mathrm{d}t} = 0. \tag{A.7}$$

Using these transformations (A.6) with (A.7), the dynamics ((A.1) and (A.3)) become

$$\begin{aligned}
\frac{\mathrm{d}s^i}{\mathrm{d}t} &= \{s^i, s^j\}\, \partial_s^j H\big|_C + \Big(\{s^i, u^j\} - \{s^i, s^l\}\, \partial_s^l U^j\Big)\, \partial_{\tilde{u}}^j H \\
&= \{s^i, s^j\}\, \partial_s^j H\big|_C + \{s^i, \tilde{u}^j\}\, \partial_{\tilde{u}}^j H \\
0 = \frac{\mathrm{d}\tilde{u}^i}{\mathrm{d}t} &= \Big(\{u^i, s^j\} - \partial_s^k U^i\, \{s^k, s^j\}\Big)\, \partial_s^j H\big|_C + \\
&\Big(\{u^i, u^j\} - \partial_s^k U^i\, \{s^k, u^j\} - \{u^i, s^k\}\, \partial_s^k U^j + \partial_s^k U^i \{s^k, s^l\} \partial_s^l U^j\Big)\, \partial_{\tilde{u}}^j H \\
&= \{\tilde{u}^i, s^j\}\, \partial_s^j H\big|_C + \{\tilde{u}^i, \tilde{u}^j\}\, \partial_{\tilde{u}}^j H.
\end{aligned} \tag{A.8}$$

We rewrite the last equation in (A.8) as

$$L^{ij}\, \partial_{\tilde{u}}^j H = -\{\tilde{u}^i, s^j\}\, \partial_s^j H\big|_C \tag{A.9}$$

with the skew-symmetric matrix

$$L^{ij} = \{\tilde{u}^i, \tilde{u}^j\}. \tag{A.10}$$

Let L^{ij} be invertible (*cf.*, the assumption stated above), which implies that L has an even number of rows and columns. After using (A.10) to reorder (A.8), the dynamics on the constrained manifold becomes

$$\frac{\mathrm{d}s^i}{\mathrm{d}t} = \Big(\{s^i, s^j\} - \{s^i, \tilde{u}^k\}\, (L^{-1})^{kl}\, \{\tilde{u}^l, s^j\}\Big)\, \partial_s^j H \tag{A.11}$$

with the associated Dirac bracket (Dirac, 1964)

$$\{F, G\}_C = \partial_s F \left(\{s, s\} - \{s, \tilde{u}\}\, L^{-1}\, \{\tilde{u}, s\}\right) \partial_s G, \tag{A.12}$$

where we have dropped the reference to the constrained derivatives and where we have substituted $\tilde{u} = 0$ in the Hamiltonian and the resulting Dirac bracket. Note that the bracket (A.12) is antisymmetric. Dirac (1958) proved that the bracket (A.12) satisfies the Jacobi identity for a canonical Poisson bracket, but this proof can be extended given any generalized Poisson bracket $\{\cdot, \cdot\}$.

Hence, we have proven our original claim (a) in the Appendix' introduction that slaved Hamiltonian dynamics leads to Hamiltonian dynamics on a constrained manifold with a Dirac bracket, under the assumption that the matrix of the bracket $\{\tilde{u}^i, \tilde{u}^j\}$ of constraints (A.4) is invertible.

(b) Leading-order Hamiltonian slow dynamics

In many applications one encounters problems with two time scales in which the dependent variables $\mathsf{z} = (s, u)$ can be divided into slow variables s and fast variables f. This division may arise after a suitable scaling of the physical problem considered, and often involves a transformation of the original variables (Van Kampen, 1985).

Hence, the formulation

$$\frac{\mathrm{d}\mathsf{z}^i}{\mathrm{d}t} = \{\mathsf{z}^i, H\} = \{\mathsf{z}^i, \mathsf{z}^j\}(\partial H/\partial \mathsf{z}^j) \tag{A.13}$$

can be written in terms of variables s and f. The bracket $\{\mathsf{z}^i, \mathsf{z}^j\}$ is by assumption given by

$$\begin{aligned}
\{s^i, s^j\} &= J^{ij}(s, f) = J_0^{ij}(s) + \varepsilon J_1^{ij}(s, f; \varepsilon)\\
\{f^i, s^j\} &= K^{ij}(s, f) = K_0^{ij}(s, f) + \varepsilon K_1^{ij}(s, f; \varepsilon)\\
\{f^i, f^j\} &= -\frac{1}{\varepsilon}T^{ij} + Y^{ij}(s, f) = -\frac{1}{\varepsilon}T^{ij} + Y_0^{ij}(s, f; \varepsilon)
\end{aligned} \tag{A.14}$$

in which we introduced functions $J = J(s, f)$, $K = K(s, f)$ and $Y = Y(s, f)$ of the slow and fast variables s and f, as indicated, and a constant invertible skew-symmetric matrix T. In detail, the dependency indicated means that $J = J(s^1, \ldots, s^{p_s}, f^1, \ldots, f^q)$ and so forth. Note that antisymmetry of the Poisson bracket dictates that $\{s, f\} = -K^{\mathrm{T}}$, where the superscript $^{\mathrm{T}}$ denotes matrix transpose. Here and in the rest of this appendix, J_0, T, Y_0, and also A and R_0 introduced below are understood to denote fixed *functions* of their arguments.

Remark 1: That J_0 cannot depend on f can be seen by considering the Jacobi identity $\{s, \{s, f\}\} + \{f, \{s, s\}\} + \{s, \{f, s\}\} = 0$ at $\mathcal{O}(1/\varepsilon)$ and in particular by considering the $\mathcal{O}(1/\varepsilon)$ term in $\{f, \{s, s\}\}$ using the form (A.14) of the bracket.

We take $H(\mathsf{z}; \varepsilon)$ of the form

$$H(s, f; \varepsilon) = \tfrac{1}{2} f^{\mathrm{T}} A\, f + R_0(s) + \varepsilon R_1(s, f; \varepsilon), \tag{A.15}$$

where A is a constant symmetric matrix. Hence, (A.13) and the Poisson bracket (A.14) imply equations of motion of the generic form

$$\frac{\mathrm{d}s}{\mathrm{d}t} = J\, \partial_s H - K^{\mathrm{T}}\, \partial_f H \quad \text{and} \quad \frac{\mathrm{d}f}{\mathrm{d}t} = K\, \partial_s H - \frac{1}{\varepsilon}\Gamma A^{-1}\, \partial_f H + Y\, \partial_f H \tag{A.16}$$

with $T=\Gamma A^{-1}$ and Γ a constant invertible skew-hermitian matrix (or a linear operator with purely imaginary eigenvalues). The latter property implies that f undergoes rapid energy-conserving oscillations in the limit $\varepsilon\to 0$. Hence the fast motions are waves, not damped motion; this property distinguishes the present approach from centre manifold theory (Carr, 1981).

Following Van Kampen (1985), we can define the constraints

$$\tilde{u}=f-U(s)=0. \tag{A.17}$$

Otherwise stated, f is slaved to s. In general, $U(s)$ is determined by expanding the fast variable f into a power series in ε or by iterating f, in both cases with s as the independent variable. Clearly at leading order, or as the leading iteration, we find $f=U_0(s)=0$ from (A.15) and (A.16), or $\tilde{u}_0=0$ from (A.17). Transforming to the variables $\{s,\tilde{u}\}$, we find the skew-symmetric matrix L^{ij} defined in (A.10) to be

$$\begin{aligned} L^{ij} &= \{f^i,f^j\}-\partial_s^k U^i\,\{s^k,f^j\}-\{f^i,s^k\}\,\partial_s^k U^j+\partial_s^k U^i\{s^k,s^l\}\partial_s^l U^j\\ &= -\frac{1}{\varepsilon}T^{ij}+Y_0^{ij}(s,f;\varepsilon)+\partial_s^k U^i\left(K_0^{jk}+\varepsilon K_1^{jk}\right)-\\ &\qquad \left(K_0^{ik}+\varepsilon K_1^{ik}\right)\partial_s^k U^j+\partial_s^k U^i\left(J_0^{kl}+\varepsilon J_1^{kl}\right)\partial_s^l U^j. \end{aligned} \tag{A.18}$$

Hence, $L^{-1}\to 0$ in the limit $\varepsilon\to 0$, since

$$(L^{-1})^{ij}=-\varepsilon\,(T^{-1})^{ij}+\mathcal{O}(\varepsilon^2). \tag{A.19}$$

At leading order, we thus find $\partial H/\partial\tilde{u}=0$ by combining (A.9) and (A.19). The Hamiltonian slow dynamics on the constrained manifold $f=0$, at leading order, is therefore

$$\frac{\mathrm{d}s}{\mathrm{d}t}=J_0\,\partial_s H_0 \tag{A.20}$$

with the leading-order Hamiltonian $H_0(s)=R_0(s)$, *cf.*, (A.15). The associated bracket is

$$\{F,G\}_0=\partial_s F\;J_0(s)\partial_s G. \tag{A.21}$$

The Jacobi identity $\{s,\{s,s\}\}+\cdots=0$ evaluated at $\mathcal{O}(1)$ only involves $J_0(s)$ as we stated in **Remark 1** in this section.

Hence, we have proven our claim (b) in the Appendix' introduction that the leading-order dynamics in a singular perturbation [of the system (A.13)–(A.15)] is Hamiltonian with a (Dirac) bracket [(A.21)] satisfying the Jacobi identity.

References

Allen, J.S. and Holm, D.D. 1996 'Extended-geostrophic Hamiltonian models for rotating shallow water motion'. *Physica D* **98**, 229–248.

Birner, T., Dörnbrack, A. and Schumann, U. 2002 'How sharp is the tropopause at midlatitudes'? *Geophys. Res. Lett.* **29**, 10.1029.

Birner, T. 2006 'The fine-scale structure of the extratropical tropopause region'. *J. Geophys. Res.* **111**, D04104.

Bokhove, O. 2002a 'Eulerian variational principles for stratified hydrostatic equations'. *J. Atmos. Sci.* **59**, 1628–1659.

Bokhove, O. 2002b 'Balanced models in Geophysical Fluid Dynamics: Hamiltonian formulation, constraints and formal stability.' In: J. Norbury, I. Roulstone (Eds.), Large-Scale Atmosphere-Ocean Dynamics: Geometric Methods and Models, Vol. 2, Cambridge University Press, Cambridge, 368 pp.

Bokhove, O. and Oliver, M. 2006 'Parcel Eulerian-Lagrangian fluid dynamics for rotating geophysical flows'. *Proc. Roy. Soc. A* **462**, 2563–2573.

Bokhove, O. and Oliver, M. 2007 'Hamiltonian Three-Layer Models for Atmospheric Dynamics'. Submitted *Q. J. Roy. Met. Soc.*

Carr, J. 1981 'Applications of centre manifold theory'. Springer, 142 pp.

Charney, J., Fjortoft, R., & Von Neumann, J. 1950 'Numerical integration of the barotropic vorticity equation'. *J. Meteorology* **1**, 237–254.

Daley, R. 1991 'Atmospheric data analysis'. Cambridge Atmospheric and Space Science Series. 457 pp.

Dirac, P.A.M. 1958 'Generalized Hamiltonian dynamics'. *Proc. Roy. Soc. Lond. A* **246**, 326–332.

Dirac, P.A.M. 1964 *Lectures on Quantum Mechanics*. Belfer Graduate School of Science, Yeshiva University, 87 pp.

Gill, A.E. 1982 'Atmosphere-Ocean Dynamics'. Academic Press, Toronto, 662 pp.

Kampen, Van, N.G. 1985 'Elimination of fast variables'. *Physics Rep.* **124**, 69–160.

Lorenz, E. 1960 'Energy and numerical weather prediction'. *Tellus* **12**. 364–373.

McIntyre, M.E. and Roulstone, I. 2002 'Are there higher-accuracy analogues of semi-geostrophic theory?' In: J. Norbury, I. Roulstone (Eds.), Large-Scale Atmosphere-Ocean Dynamics: Geometric Methods and Models, Vol. 2, Cambridge University Press, Cambridge, 368 pp.

Ripa, P. 1993 'Conservation laws for primitive equations with inhomogeneous layers'. *Geophys. Astrophys. Fluid Dyn.* **70**, 85–111.

Olver, P.J. 1986 'Applications of Lie groups to differential equations.' Springer, 497 pp.

Salmon, R. 1985 'New equations for nearly geostrophic flow'. *J. Fluid Mech.* **153**, 461–477.

Salmon, R. 1988 'Semigeostrophic theory as a Dirac-bracket projection'. *J. Fluid Mech.* **196**, 345–358.

Salmon, R. 1998 'Lectures on geophysical fluid dynamics', Oxford University Press. 192 pp.

Shepherd, T. G. 1990 'Symmetries, conservation laws, and Hamiltonian structure in geophysical fluid dynamics'. *Adv. Geophys.* **32**, 287–338.

Shepherd, T. G. 1993 'A unified theory of available potential energy'. *Atmos.-Ocean* **31**, 1–26.

Starr, V.P. 1945 'A quasi-Lagrangian system of hydrodynamical equations'. *J. Meteorol.* **2**, 227–237.

Trieling, R.R. and Verkleij, W.T.M. 2002 'Synoptic development in a two-and-a-half layer contour dynamics system'. *J. Atmos. Sci.* **60**, 913–935.

Vanneste, J. and Bokhove, O. 2002 'Dirac bracket approach to nearly geostrophic Hamiltonian balanced models'. *Physica D* 164, 152–167.

Vanneste J. 2004 'Inertia-gravity-wave generation by balanced motion: revisiting the Lorenz-Krishnamurthy model'. *J. Atmos. Sci.* **61**, 224–234.

Vanneste J. and Yavneh, I. 2004 'Exponentially small inertia-gravity waves and the breakdown of quasi-geostrophic balance'. *J. Atmos. Sci.* **61**, 211–223.

Verkley, W.T.M. 2001 'Salmon's Hamiltonian approach to balanced flow applied to a one-layer isentropic model of the atmosphere'. *Quart. J. Roy. Meteor. Soc.* **127**, 579–600.

Warn, T., O. Bokhove, T. G. Shepherd, and G. K. Vallis 1995 'Rossby-number expansions, slaving principles and balance dynamics'. *Quart. J. Roy. Meteor. Soc.* **121**, 723–739.